Thin film diamond thermistors for space environment applications

M.A. Neto[1,*], S. Pratas[1], E.L. Silva[1], A.V. Girão[1], F.J. Oliveira[1], R.F. Silva[1]

[1] Department of Materials and Ceramic Engineering, CICECO – Aveiro Institute of Materials, University of Aveiro. 3810-193, Aveiro, Portugal
**Corresponding author: mangelo@ua.pt*

ABSTRACT

Temperature sensors for space exploration not only have to be capable to withstand high fluctuating temperatures but must be radiation proof, be mechanically tough to handle the extreme G-forces during their launch to space and be oxidation resistant, while maintaining their thermal sensitivity and stability over a wide temperature interval.

The novel thermistors proposed here are based on boron-doped diamond (BDD) and undoped diamond (UND) thin films grown on silicon nitride (Si_3N_4) ceramic substrates and are aimed at addressing the shortcomings of current space-qualified temperature sensors. The selected planar geometry will maximize the thermal contact area. Since the temperature sensitive film of the thermistor is made of diamond, the best thermal conductor material, and is just a few micrometres thick, it will give incredibly fast response times to small temperature variations, with great thermal stability.

Another innovative aspect of these diamond thermistors is their ability to measure temperature without contact. Our preliminary work has demonstrated the electrical response of these sensors to small temperature variations by infrared radiation. This feature is important in applications where thermal contact with the sensor is not possible or undesirable such as measuring the temperature of sensitive and rotating mechanical parts and components in the vacuum of space.

INTRODUCTION

One of the most crucial aspects of space exploration is the constant necessity to monitor temperature, correctly and quickly, of essential components of particular equipment. However, space is a very unique and harsh environment, characterized by very low atmospheric pressure and constant exposure to infrared and ionizing radiation. Thus, space qualified temperature sensors must be capable to withstand high fluctuating temperatures and be radiation proof, while maintaining their thermal sensitivity over a wide temperature interval. Furthermore, such sensors must be mechanically tough to handle the extreme mechanical loads during their launch to space, and oxidation resistant to properly handle the typical and extreme oxidative environment of the LEO (Low Earth Orbit) region. As a result, these sensors must satisfy, not only one, but a complete set of outstanding physical, mechanical and chemical properties.

Negative Temperature Coefficient (NTC) thermistors are semiconductors whose electrical resistance decreases with increasing temperature. This class of temperature sensors is widely used in space applications for constant and accurate temperature monitoring since they have fast response times and high thermal sensitivity. The most common and commercially available thermistors are based on transition metal oxides with application limited to a few hundred degrees. However, with some modifications to their composition and structure, these thermistors can be used in temperatures up to 1000°C [1–3]. Thermistors based on SiC can operate in environments up to 500°C [4]. However, almost all these temperature sensors are mechanically fragile, show low chemical inertness and their thermal response declines with continuous exposure to ionizing radiation. Consequently, manufacturers began producing encapsulated thermistors to increase their mechanical toughness and chemical inertness, and prevent electric interaction with the surrounding environment. Some examples include thermistors with encapsulation materials such as glass, stainless steel, gold, epoxy resin and silicon-based elastomers RTV (Room Temperature Vulcanized). Variohm Eurosensor has ESA/ESSC certified thermistors for space exploration, featuring a variety of sensors for incorporation into printed circuit boards (PCBs), with and without gold coating [5]. SpaceTech GmbH Immenstaad (STI) has platinum thermistors also certified for space exploration and based on the PT1000 standard, without encapsulation and encapsulated with Kapton film and RTV [6]. TE Connectivity has a variety of encapsulated NTC thermistors, mainly with epoxy and glass [7], including NASA qualified thermistors for space applications in the temperature range from -55°C to 150°C [8]. Nevertheless, most of these sensors are unable to withstand large mechanical loads or cope with very wide temperature fluctuations and still maintain their operability under ionized radiation (x-rays, gamma, protons and neutrons) with fast response times, high thermal sensitivity and stability. Their response, thermal sensitivity and stability are thus expected to degrade with time and, eventually, resulting in the premature termination of the space mission. Therefore, as

humanity intensifies its presence in space, there is a greater need for temperature sensors that can effectively operate in such environment for longer periods of time.

Diamond is considered the ultimate material with exceptional physical and chemical properties. It has the highest thermal conductivity, high dielectric constant when free of dopants but it turns into a p-type or n-type semiconductor when doped with boron or phosphorous, respectively [9, 10]. Its low friction coefficient, extreme hardness, and chemical inertness, makes diamond an exceptional material for many demanding applications [11, 12]. Pure diamond has exceptional high transmission over a very broad range of wavelengths, including IR, visible, long and short UV, X-rays and gamma radiation. Yet, the presence of defects and impurities in CVD diamond may induce optical absorption [31]. The first NTC thermistors based on boron-doped CVD (Chemical Vapor Deposition) diamond (BDD) were developed in the 80's/90's and were able to operate at temperatures within the range 500–700°C [13, 14] without encapsulation and up to 1000°C [15], once encapsulated. On the other hand, silicon nitride (Si_3N_4) base ceramics are some of the best materials for the growth of CVD diamond, resulting in good quality and adherent films [16-18]. These ceramics show a combination of mechanical and thermal properties that leads to an exceptional ability to withstand high structural loads, even at high temperature with increased wear abrasive resistance [19–21].

Thermistors for use in space also require good quality and well adhered electrical contacts with low ohmic resistivity that can endure the hazardous conditions of such extreme environment. This guarantees the sensor's operability with minimal power losses and performance degradation. High-quality contacts on diamond may be obtained using various combinations of ion implantation [22], metal deposition and annealing techniques [23–26]. For example, by evaporating or sputtering sequential layers of Ti, Pt and Au onto the diamond surface, with subsequent annealing above 500 °C, it is possible to create ohmic contacts. Also, nearly-ohmic contacts can be fabricated on BDD by evaporating a metallic titanium layer onto the substrate prior to the diamond growth [27]. Ti/Au ohmic contacts were also successfully fabricated on NTC BDD thermistors grown on Si_3N_4 ceramics [28] but little is said about the operation limits with respect to temperature, pressure, mechanical loads and radiation. Recently, a new method to produce electric contacts on CVD diamond and Si_3N_4 ceramics was presented [29]. These contacts are expected to operate under severe conditions due to a hybrid WC-diamond region formed during the diamond growth phase [30]. Furthermore, our latest work has demonstrated the electric sensitivity of these diamond thermistors to IR radiation [31]. Therefore, we propose the use of diamond thermistors as resilient temperature sensors, either in thermal contact or contactless applications in the space environment.

EXPERIMENTAL

1. Thermistor fabrication

Diamond thermistors were fabricated on 3x3x1 mm^3 dielectric β-Si3N4 ceramic substrates, in a homemade Hot-Filament Chemical Vapor Deposition (HFCVD) reactor. These ceramics were prepared using a standard pressureless sintering process optimized in our research group [32]. The sintered bodies were then cut and ground to the desired dimensions with a diamond coated disk and grinding wheel, respectively. The substrates were then polished using three consecutive steps with 15 μm, 6 μm diamond grit and colloidal silica (0.05 μm) to a mirror-like finish (surface roughness parameter, Ra ≈ 0.008 μm). The high diamond film adhesion to the ceramic substrate is guaranteed by applying a CF_4 plasma etching treatment to the polished substrates [33]. Finally, to increase diamond nucleation, the substrates were ultrasonically abraded for 30 min in a suspension of 99.9% pure ethanol and 0.5–1 μm diamond powder. Two NTC diamond surfaces on Si_3N_4 were grown for 3 h in the HFCVD reactor, using the process parameters presented in Table 1 and keeping the ceramic substrates at a constant temperature between 750 and 800 °C.

Table 1. HFCVD growth conditions for the NTC diamond layer for the two diamond thermistors.

Thermistor	CH_4/H_2 flow ratio	Ar flow (ml/min)	Pressure (mbar)	T_f (°C)
TA	0.023	5	100	2200
TB	0.038	5	75	2190

The fabrication method, described in our previous work [29], can be visualized and easily understood by observation of the cross-section structure diagram of the thermistor presented in Fig. 1. First, on the diamond abraded surface of the ceramic substrate (1), the NTC boron doped microcrystalline diamond (BDD) layer was grown (2) using the experimental conditions given in Table 1. Then, the substrates were turned upside down and placed again in the

HFCVD chamber, with the non-diamond coated surface facing a new set of clean, non-carburized tungsten filaments. These filaments were then heated for 2–4 min, under primary vacuum (≈5 × 10−2 mbar), keeping a filament temperature between 1500 and 1900 °C. The thickness of the tungsten evaporated layer (3) depends on the temperature, length, diameter, and number of filaments used as well as on their evaporation time. After adding hydrogen and methane to the HFCVD system a WC film is created leading to a hybrid diamond-WC layer. Next, two separate electrodes were created on the back side of the thermistor using a groove (4), which divides the tungsten carbide layer in two independent parts, i.e. contact electrodes. Finally, the boron doped diamond layer was isolated and prevented from interacting with the surrounding environment through a final CVD deposition step. In this case, an undoped CVD diamond layer (5) was grew on top of the BDD for 1 h, using the growth parameters: 200 ml/min of total gas flow; 3.5% CH_4 in H_2; 50 mbar chamber pressure; substrate temperature around 750–800 °C; and filament temperature between 2100 and 2150 °C. Finally, electrical signal of the NTC surface was measured by fixing two copper wires onto the contact electrodes using high conductivity silver paint (6).

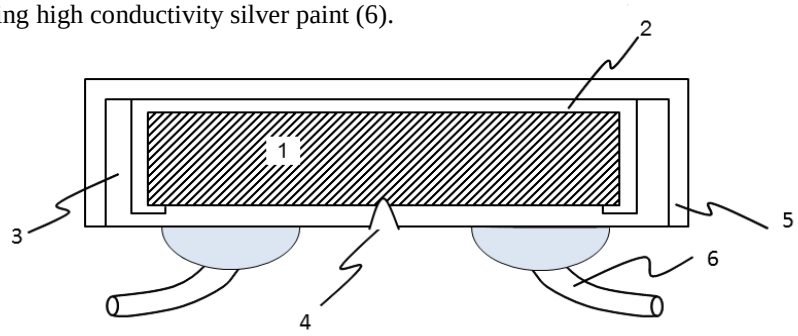

Figure 1 - Cross-section view of our NTC diamond thermistors.

2. Thermal contact testing

The performance of the diamond thermistors was evaluated by measuring their electrical resistance dependence within the temperature interval 25-425 ºC, when placed in direct contact with a type-K thermocouple controlled heating plate. This was done at atmospheric pressure using a DASYLAB based software and signal acquisition hardware that enabled the control of the heating rate at a constant value of 5 ºC/min.

3. Contactless testing

For contactless testing, the TA thermistor was glued with silver paste onto a PCB using the two WC contacts (Figure 2). To assess if it is possible to use our diamond thermistors to detect temperature variation by infrared (IR) radiation, we have placed the TA thermistor as close as possible to a diamond coated carbide tool used for face milling of an Inconel 718 workpiece (Figure 3). The detailed testing conditions can be found in this work [34]. During the machining process, the temperature of the tool tip was monitored simultaneously by the TA thermistor and by an IR thermographic camera (FLIR Systems, Wilsonville, OR, USA.). The maximum temperature plot registered by the IR camera was then correlated with the voltage output registered by the diamond thermistor over the machining time.

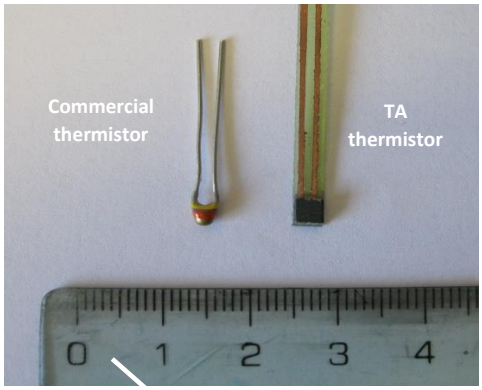

Figure 2- Side-by-side comparison between a typical commercial thermistor (at left) and our TA diamond thermistor (at right).

Face milling of the workpiece was performed in a back-and-forth linear motion in the X-Y plane, without increment in the Z direction, and with the tool permanently within the boundaries of the workpiece. During the machining process, simultaneous temperature monitoring was performed by IR thermography and by the TA thermistor. The IR thermographic camera was placed 30 cm away from the tool, with the emissivity set to 0.95, allowing the calibration of the thermistor in terms of voltage-temperature variation, and response time as well.

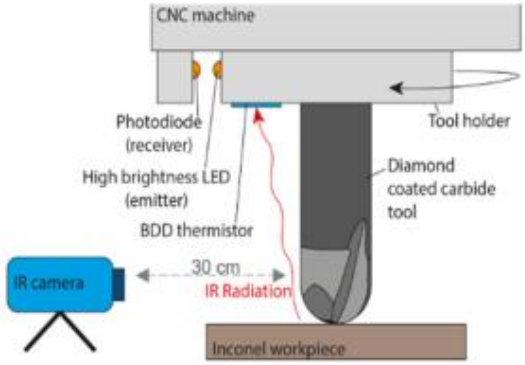

Figure 3- Overall setup for simultaneous contactless temperature monitoring with the IR camera and TA thermistor during face milling of the Inconel 718 workpiece.

RESULTS

The graph of Figure 4a) illustrates the V-I characteristic curves of thermistor TA in thermal contact with the heating plate at room pressure and at various temperatures. The experimental data presented in the graph shows that there is a linear dependence of the thermistor electrical current as a function of the applied voltage, from room temperature up to 425 ºC. Furthermore, with increasing temperature there is an increase of the current for the same applied voltage. This implies that the electrical resistance of these thermistors decreases with temperature – the typical behavior of NTC thermistors.

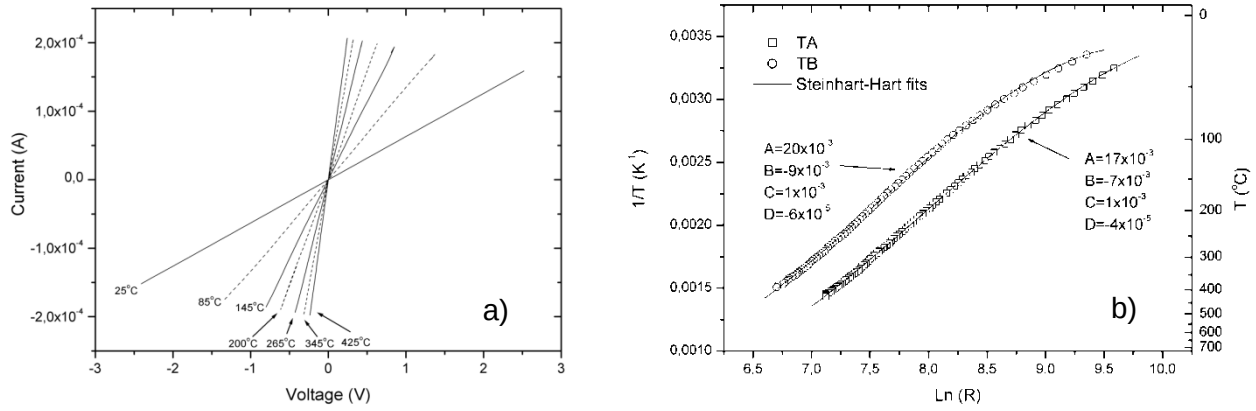

Figure 4 – a) V-I characteristic curves of thermistor TA at different temperatures; b)

When plotting the electrical resistance as a function of temperature, we found a non-linear behavior for both thermistors TA and TB, as evidenced by the graph in Figure 4b). Then, using the third order polynomial Steinhart and Hart equation (Eq. 1) [35] we have fitted the experimental data and obtained the thermistors parameters A, B, C e D.

$$1/T = A + B*\ln(R) + C*\ln(R)2 + D*\ln(R)3 \qquad \text{(Eq. 1)}$$

The calculated Steinhart and Hart parameters, presented in the graph (Figure 4b), show that the two thermistors have very similar constants. However, for TA, the A and B parameters are slightly higher when compared to those for TB, which justifies its higher resistance over the entire temperature range (i.e. @25 ºC, ~15 kΩ for TA and ~13 kΩ for TB; @425 ºC, ~1.7 kΩ for TA and ~0.7 kΩ for TB).

It is also common to approximate Eq.1 to a first order polynomial, taking into account the first two terms and specifying temperature intervals where the dependence between Ln(R) and 1/T is approximately linear. Therefore, it is valid to determine the beta (β) parameter (Eq. 2) using the electrical resistance measured at two different temperatures. In this equation, the β parameter quantifies the thermal sensitivity of the thermistor.

$$\beta = \ln(R1/R2)/(1/T1-1/T2) \qquad \text{(Eq. 2)}$$

The β parameter was calculated for both thermistors, considering two different temperature ranges of 25-85 ºC and 85-425 ºC. In the first one, β was 1700 K and 2000 K for TA and TB, respectively; in the second temperature range, β was 1250 K for TA and 1200 K for TB. These results show that the thermal sensitivity of both thermistors is considerably lower for the higher temperature interval. In addition, TB is significantly more sensitive at lower temperature when compared to TA, giving a slightly higher β value at higher temperature. Nonetheless, the obtained β values are within the range reported for other diamond-based thermistors (1000-5500 K) [36-38]. The observed difference for the β values found for both thermistors can be explained by the combined effect of methane content and chamber pressure during the CVD growth of the boron doped diamond layer. According to Table 1, TA was grown under higher H_2 content and system pressure. It is well known that the increase of hydrogen content preferentially stabilizes sp^3 carbon hybridization on the growing diamond surface resulting in better diamond crystallinity and bigger diamond grains. In turn, this process favors boron doping thus leading to increased conductivity and then affecting the β parameter. On the other side, the increase of pressure can be understood as increasing the residence time of the chemical growth species inside the chamber. As a result, and in analogy with another work [39], for this particular doping system with boron oxide and ethanol added to the gas phase, the negative effect of oxygen species on boron incorporation would be higher when higher pressure is used. Thus, by adjusting the HFCVD growth parameters for the BDD layer it is possible to control the thermal sensitivity of the diamond thermistors. This could be useful for the development of tailored temperature sensors for very specific contact applications.

For the contactless experiment, Figure 4 shows a remarkable correspondence between the temperature registered by thermal imagery and the voltage measured by the amplification setup with wireless connection to the TA thermistor. The plot shows the highest temperatures were registered at the end mill tip when the tool reached inflection positions at both the extremities of the cutting path, and lowest temperatures were registered at mid path position. Since the end mill tool is at constant rotation, we can conclude that the IR radiation from the carbide tool greatly influences the electrical response of the diamond thermistor. Moreover, there is a fast response time of the diamond thermistor when the milling tool changes rapidly its temperature.

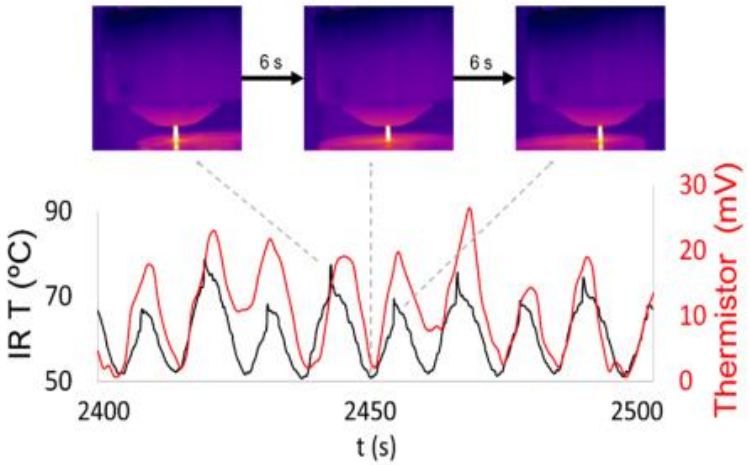

Figure 5 – Time dependent plot for the temperature of the end mill tool recorded by the thermographic camera showing lower temperature at the tool tip when at the middle of the cutting path and higher temperature at inflection positions. Superimposed TA thermistor signal, after amplification, displaying a response closely matched the response time of the thermographic camera.

CONCLUSIONS

The new thin films diamond thermistors, presented in this work demonstrated the ability to measure temperature over a wide range. Furthermore, the fabricated thermistors planar geometry and small size maximizes the contact region between the temperature sensitive surface and any solid flat surface on which they may be placed for measurements. This enables improved response times when compared to the traditional round shaped thermistors. The thermal sensitivity parameter (β) obtained for our thermistors are well within the range of values obtained for other CVD diamond-based and non-diamond thermistors. Moreover, tailored diamond thermistors are easily obtained using the methodology presented here. In fact, by tuning certain HFCVD growth parameters it is possible to control the β parameter for a specific temperature interval.

These diamond thermistors have also the ability to measure temperature without contact with very fast response times. This feature is very important for thermal sensors when it is crucial to monitor the temperature of moving parts and components where the contact is not possible.

The diamond-Si_3N_4 platform used for the thermistor fabrication will guarantee superior mechanical toughness and chemical inertness that, in their turn, allow this type of electronic component to be used for temperature measurements under extreme conditions, such as those found in space.

ACKNOWLEDGEMENTS

This work was developed within the scope of the project CICECO-Aveiro Institute of Materials, UIDB/50011/2020, UIDP/50011/2020 & LA/P/0006/2020, financed by national funds through the FCT/MEC (PIDDAC). This work was also funded by national funds (OE) through FCT – Fundação para a Ciência e a Tecnologia, I.P., in the scope of the framework contract foreseen in the numbers 4, 5 and 6 of the article 23, of the Decree-Law 57/2016, of August 29, changed by Law 57/2017, of July 19 and financed by Portugal 2020 through European Regional Development Fund (ERDF) in the frame of Operational Competitiveness and Internationalization Program (POCI) and in the scope of the project DHardTools (POCI-01-0247-FEDER-039538).

REFERENCES

[1] Feteira, A. (2009). Negative Temperature Coefficient Resistance (NTCR) Ceramic Thermistors: An Industrial Perspective. In Journal of the American Ceramic Society (Vol. 92, Issue 5, pp. 967–983). Wiley. https://doi.org/10.1111/j.1551-2916.2009.02990.x

[2] Kulawik, J., Szwagierczak, D., Gröger, B., & Skwarek, A. (2007). Fabrication and characterization of bulk and thick film perovskite NTC thermistors. In Microelectronics International (Vol. 24, Issue 2, pp. 14–18). Emerald. https://doi.org/10.1108/13565360710745548

[3] Feltz, A., & Pölzl, W. (2000). Spinel forming ceramics of the system FexNiyMn3–x–yO4 for high temperature NTC thermistor applications. In Journal of the European Ceramic Society (Vol. 20, Issues 14–15, pp. 2353–2366). Elsevier BV. https://doi.org/10.1016/s0955-2219(00)00140-0

[4] Nagai, T., & Itoh, M. (1990). SiC thin-film thermistors. In IEEE Transactions on Industry Applications (Vol. 26, Issue 6, pp. 1139–1143). Institute of Electrical and Electronics Engineers (IEEE). https://doi.org/10.1109/28.62400

[5]https://www.variohm.com/products/temperature-sensors/space-qualified-hi-rel-thermistors

[6] https://www.spacetech-i.com/products/electronics-sensors/thermistors

[7] https://www.te.com/usa-en/products/sensors/temperature-sensors/ntc-thermistors-sensors.html

[8] https://www.te.com/usa-en/trends/smart-connectivity-for-smart-cities/sensors-in-space.html

[9] Gajewski, W., Achatz, P., Williams, O. A., Haenen, K., Bustarret, E., Stutzmann, M., & Garrido, J. A. (2009). Electronic and optical properties of boron-doped nanocrystalline diamond films. In Physical Review B (Vol. 79, Issue 4). American Physical Society (APS). https://doi.org/10.1103/physrevb.79.045206

[10] Pinault, M.-A., Barjon, J., Kociniewski, T., Jomard, F., & Chevallier, J. (2007). The n-type doping of diamond: Present status and pending questions. In Physica B: Condensed Matter (Vols. 401–402, pp. 51–56). Elsevier BV. https://doi.org/10.1016/j.physb.2007.08.112

[11] May, P. W. (2000). Diamond thin films: a 21st-century material. In J. M. T. Thompson (Ed.), Philosophical Transactions of the Royal Society of London. Series A: Mathematical, Physical and Engineering Sciences (Vol. 358, Issue 1766, pp. 473–495). The Royal Society. https://doi.org/10.1098/rsta.2000.0542

[12] Blank, V. D., Buga, S. G., Bormashov, V. S., Terentiev, S. A., Kuznetsov, M. S., Nosukhin, S. A., & Pel', E. G. (2007). Pulse thermometers based on synthetic single crystal boron-doped diamonds. In Diamond and Relat. Mater. (Vol. 16, Issues 4–7, pp. 970–973). Elsevier BV. https://doi.org/10.1016/j.diamond.2006.12.049

[13] Bade, J. P., Sahaida, S. R., Stoner, B. R., von Windheim, J. A., Glass, J. T., Miyata, K., Nishimura, K., & Kobashi, K. (1993). Fabrication of diamond thin-film thermistors for high-temperature applications. In Diamond and Relat. Mater. (Vol. 2, Issues 5–7, pp. 816–819). Elsevier BV. https://doi.org/10.1016/0925-9635(93)90230-y
[14] Kim, T. J., Davis, K. L., Liu, Y., Bredemann, J. R., Ma, Z., Anderson, M., & Corradini, M. L. (2019). Development of a Stable High-Temperature Diamond Thermistor Using Enhanced Supporting Designs. In IEEE Sensors Journal (Vol. 19, Issue 16, pp. 6587–6594). Institute of Electrical and Electronics Engineers (IEEE). https://doi.org/10.1109/jsen.2019.2912566
[15] Aslam, M., Yang, G. S., & Masood, A. (1994). Boron-doped vapor-deposited diamond temperature microsensors. In Sensors and Actuators A: Physical (Vol. 45, Issue 2, pp. 131–137). Elsevier BV. https://doi.org/10.1016/0924-4247(94)00830-2
[16] Belmonte, M., Fernandes, A. J. S., Costa, F. M., Oliveira, F. J., & Silva, R. F. (2003). Adhesion behaviour assessment on diamond coated silicon nitride by acoustic emission. In Diamond and Relat. Mater. (Vol. 12, Issues 3–7, pp. 733–737). Elsevier BV. https://doi.org/10.1016/s0925-9635(02)00305-9
[17] Amaral, M., Oliveira, F. J., Belmonte, M., Fernandes, A. J. S., Costa, F. M., & Silva, R. F. (2003). Tailored Si3N4Ceramic Substrates for CVD Diamond Coating. In Surface Engineering (Vol. 19, Issue 6, pp. 410–416). Informa UK Limited. https://doi.org/10.1179/026708403225010136
[18] Neto, M. A., Silva, E. L., Ghumman, C. A., Teodoro, O. M., Fernandes, A. J. S., Oliveira, F. J., & Silva, R. F. (2012). Composition profiles and adhesion evaluation of conductive diamond coatings on dielectric ceramics. In Thin Solid Films (Vol. 520, Issue 16, pp. 5260–5266). Elsevier BV. https://doi.org/10.1016/j.tsf.2012.03.049
[19] Belmonte, M., Miranzo, P., Osendi, M. I., & Gomes, J. R. (2009). Wear of aligned silicon nitride under dry sliding conditions. In Wear (Vol. 266, Issues 1–2, pp. 6–12). Elsevier BV. https://doi.org/10.1016/j.wear.2008.05.004
[20] Wasanapiarnpong, T., Wada, S., Imai, M., & Yano, T. (2006). Effect of post-sintering heat-treatment on thermal and mechanical properties of Si3N4 ceramics sintered with different additives. In Journal of the European Ceramic Society (Vol. 26, Issue 15, pp. 3467–3475). Elsevier BV. https://doi.org/10.1016/j.jeurceramsoc.2005.10.011
[21] Mehrotra, P. K. (1997). Applications of Ceramic Cutting Tools. In Key Engineering Materials (Vols. 138–140, pp. 1–24). Trans Tech Publications, Ltd. https://doi.org/10.4028/www.scientific.net/kem.138-140.1
[22] Brandes, G. R., Beetz, C. P., Feger, C. F., Wright, R. W., & Davidson, J. L. (1999). Ion implantation and anneal to produce low resistance metal–diamond contacts. In Diamond and Relat. Mater. (Vol. 8, Issue 10, pp. 1936–1943). Elsevier BV. https://doi.org/10.1016/s0925-9635(99)00161-2
[23] Moazed, K. L., Zeidler, J. R., & Taylor, M. J. (1990). A thermally activated solid state reaction process for fabricating ohmic contacts to semiconducting diamond. In Journal of Applied Physics (Vol. 68, Issue 5, pp. 2246–2254). AIP Publishing. https://doi.org/10.1063/1.346529
[24] Jany, C., Foulon, F., Bergonzo, P., & Marshall, R. D. (1998). Post-growth treatments and contact formation on CVD diamond films for electronic applications. In Diamond and Relat. Mater. (Vol. 7, Issue 7, pp. 951–956). Elsevier BV. https://doi.org/10.1016/s0925-9635(97)00332-4
[25] Looi, H. J., Pang, L. Y. S., Whitfield, M. D., Foord, J. S., & Jackman, R. B. (2000). Engineering low resistance contacts on p-type hydrogenated diamond surfaces. In Diamond and Relat. Mater. (Vol. 9, Issues 3–6, pp. 975–981). Elsevier BV. https://doi.org/10.1016/s0925-9635(00)00240-5
[26] Chen, Y., Ogura, M., Yamasaki, S., & Okushi, H. (2005). Ohmic contacts on p-type homoepitaxial diamond and their thermal stability. In Semiconductor Science and Technology (Vol. 20, Issue 8, pp. 860–863). IOP Publishing. https://doi.org/10.1088/0268-1242/20/8/041
[27] Alexander, M. S., Latto, M. N., May, P. W., Jason Riley, D., & Pastor-Moreno, G. (2003). A simple route to Ohmic contacts on low boron-doped CVD diamond. In Diamond and Relat. Mater. (Vol. 12, Issue 9, pp. 1460–1462). Elsevier BV. https://doi.org/10.1016/s0925-9635(03)00174-2
[28] Miyata, K., Saito, K., Nishimura, K., & Kobashi, K. (1994). Fabrication and characterization of diamond film thermistors. In Review of Scientific Instruments (Vol. 65, Issue 12, pp. 3799–3803). AIP Publishing. https://doi.org/10.1063/1.1144510
[29] Neto, M. A., Esteves, D., Girão, A. V., Oliveira, F. J., & Silva, R. F. (2020). Tough negative temperature coefficient diamond thermistors comprising tungsten carbide ohmic contacts. In Diamond and Relat. Mater. (Vol. 109, p. 108036). Elsevier BV. https://doi.org/10.1016/j.diamond.2020.108036
[30] Neto, M. A., Silva, E. L., Fernandes, A. J. S., Oliveira, F. J., & Silva, R. F. (2012). Diamond/WC bilayer formation mechanism by hot-filament CVD. In Surface and Coatings Technology (Vol. 206, Issue 13, pp. 3055–3063). Elsevier BV. https://doi.org/10.1016/j.surfcoat.2011.12.005
[31] Pratas, S.; Silva, E.L.; Neto, M.A.; Fernandes, C.M.; Fernandes, A.J.S.; Figueiredo, D.; Silva, R.F. “Boron Doped Diamond for Real-Time Wireless Cutting Temperature Monitoring of Diamond Coated Carbide Tools”. Materials 2021, 14, 7334. https://doi.org/10.3390/ma14237334

[32] M. Belmonte, V.A. Silva, A.J.S. Fernandes, F.M. Costa, R.F. Silva, Surface Pretreatments of Silicon Nitride for CVD Diamond Deposition, J. Am. Ceram. Soc. 86 (2003) 749-754. https://doi.org/10.1111/j.1151-2916.2003.tb03369.x
[33] F.A. Almeida, M. Amaral, F.J. Oliveira, A.J.S. Fernandes, R.F. Silva, Nano tomicrometric HFCVD diamond adhesion strength to Si3N4, Vacuum 81 (2007) 1443-1447. https://doi.org/10.1016/j.vacuum.2007.04.008
[34] Pratas, S.; Silva, E.L.; Neto, M.A.; Fernandes, C.M.; Fernandes, A.J.S.; Figueiredo, D.; Silva, R.F. "Boron Doped Diamond for Real-Time Wireless Cutting Temperature Monitoring of Diamond Coated Carbide Tools". Materials 2021, 14, 7334. https://doi.org/10.3390/ma14237334
[35] J.S. Steinhart and S.R. Hart, Calibration curves for thermistors, Deep. Sea Res. Oceanographic Abstr. 15 (1968) 497–503. https://doi.org/10.1016/0011-7471(68)90057-0
[36] J.P. Bade, S.R. Sahaida, B.R. Stoner, J.A. von Windheim, J.T. Glass, K. Miyata, K. Nishimura, K. Kobashi, Fabrication of diamond thin-film thermistors for high-temperature applications, Diamond and Rel. Mater. 2 (1993) 816-819. https://doi.org/10.1016/0925-9635(93)90230-Y
[37] T.J. Kim, K.L. Davis, Y. Liu, J.R. Bredemann, Z. Ma, M. Anderson, M. L. Corradini, Development of a Stable High-Temperature Diamond Thermistor Using Enhanced Supporting Designs IEEE Sensors Journal 19 (2019) 6587-6594. https://doi.org/10.1109/JSEN.2019.2912566
[38] T.D. McGee, Principles and Methods of Temperature Measurements, John Wiley & Sons, New York, 1988.
[39] M.A. Neto, G. Pato, N. Bundaleski, O.M.N.D. Teodoro, A.J.S. Fernandes, F.J. Oliveira, R.F. Silva, Surface modifications on as-grown boron doped CVD diamond films induced by the B2O3–ethanol–Ar system, Diamond and Relat. Mater. 64 (2016) 89-96. https://doi.org/10.1016/j.diamond.2016.02.001